Available online at www.sciencedirect.com
SCIENCE DIRECT®
Vision Research 45 (2005) 1793–1805
Vision Research
www.elsevier.com/locate/visres

"Phase capture" in amblyopia: The influence function for sampled shape

Dennis M. Levi *, Roger W. Li, Stanley A. Klein

University of California, Berkeley, School of Optometry & Helen Wills Neuroscience Institute, Berkeley, CA 94720-2020, USA

Received 8 October 2004; received in revised form 6 January 2005

Abstract

This study was concerned with what stimulus information humans with amblyopia use to judge the shape of simple objects. We used a string of four Gabor patches to define a contour. A fifth, center patch served as the test pattern. The observers' task was to judge the location of the test pattern relative to the contour. The contour was either a straight line, or an arc with positive or negative curvature. We asked whether phase shifts in the inner or outer pairs of patches distributed along the contour influence the perceived shape. That is, we measured the phase shift influence function. Our results, consistent with previous studies, show that amblyopes are imprecise in shape discrimination, showing elevated thresholds for both lines and curves. We found that amblyopes often make much larger perceptual errors (biases) than do normal observers in the absence of phase shifts. These errors tend to be largest for curved shapes and at large separations. In normal observers, shifting the phase of *inner* patches of the string by 0.25 cycle results in almost complete phase capture (attraction) at the smallest separation (2λ), and the capture effect falls off rapidly with separation. A 0.25 cycle shift of the *outer* pair of patches has a much smaller effect, in the opposite direction (repulsion). While several amblyopic observers showed reduced capture by the phase of the inner patches, to our surprise, several of the amblyopes were sensitive to the phase of the outer patches. We used linear multiple regression to determine the weights of all cues to the task: the carrier phase of the inner patches, carrier phase of the outer patches and the envelope of the outer patches. Compared to normal observers, some amblyopes show a weaker influence of the phase of the inner patches, and a stronger influence of both the phase and envelope of the outer patches. We speculate that this may be a consequence of abnormal "crowding" of the inner patches by the outer ones.

Keywords: Amblyopia; Shape perception; Psychophysics; Influence function; Cue combination; Phase perception; Classification image; Crowding

1. Introduction

Humans with normal vision have a highly acute ability to judge the shape of an object, and to identify and localize distortions in the shapes of smooth objects (e.g., Watt, Ward, & Casco, 1987; Whitaker & McGraw, 1998; Wilkinson, Wilson, & Habak, 1998; Zanker & Quenzer, 1999). Recent work suggests that when there is more than one cue to shape, each cue is given a weight based on its reliability (see Jacobs, 2002 for a recent review) and the cues are combined according to their weights. This approach explains how haptic and visual cues are combined (Ernst & Banks, 2002; Hillis, Ernst, Banks, & Landy, 2002). Other work suggests similar cue combination rules operate in other domains, e.g. stereopsis (Landy, Maloney, Johnston, & Young, 1995; Young, Landy, & Maloney, 1993), and in selective attention (Murray, Sekuler, & Bennett, 2003).

In a recent study (Levi, Li, & Klein, 2003) we used a string of four Gabor patches to define a contour. A fifth,

* Corresponding author. Tel.: +1 510 642 3414; fax: +1 510 642 7806.
E-mail address: dlevi@berkeley.edu (D.M. Levi).

0042-6989/$ - see front matter © 2005 Elsevier Ltd. All rights reserved.
doi:10.1016/j.visres.2005.01.021

center patch served as test pattern: we asked whether phase shifts in the inner or outer pairs of patches distributed along the contour, influence perceived shape. We found that shifting the *inner* patches of the string by 0.25 cycle results in almost complete phase capture (attraction) at the smallest separation (2λ), and the capture effect fell off rapidly with separation. A 0.25 cycle shift of the *outer* pair of patches had a smaller effect, in the opposite direction (repulsion). In these experiments, the contour was defined by two cues—the cue provided by the Gabor carrier (the 'carrier' cue) and that defined by the Gaussian envelope (the 'envelope' cue). Our phase shift influence function can be thought of as a cue combination task. An ideal observer would weight the cues by the inverse variance of the two cues. The variance in each of these cues predicted the main features of our results quite accurately.

Although the normal human visual system is highly sensitive to changes in phase, several studies suggest that strabismic amblyopes may be much less sensitive to spatial phase (Lawden, Hess, & Campbell, 1982; Pass & Levi, 1982). Of special relevance here is the finding that while normal observers see a strong illusion of tilt that is induced in a row of aligned Gabor patches, when a phase shift is added to successive patches (Popple & Levi, 2000a; Popple & Sagi, 2000), many amblyopes are blind or insensitive to this "phase illusion" (Popple & Levi, 2000b). Popple and Levi (2000b) favored an explanation based on an integration deficit for the failure of amblyopes to see the phase illusion (see also Simmers & Bex, 2004); however, an alternative hypothesis is that amblyopes fail to see the illusion because they are insensitive to phase shifts or because they do not apply the same weights to the phase cue as do normal observers (Popple & Levi, 2004). Insensitivity to phase shifts might provide an analog of a dichromat for spatial vision; i.e., a "phase blind" observer.

In the present study, we consider three aspects of amblyopes' shape perception: first, the precision with which amblyopes perform the task. A large number of previous studies have focused on the precision of position and shape judgments in amblyopia (e.g., Demanins & Hess, 1996; Hess, Wang, Demanins, Wilkinson, & Wilson, 1999; Levi, Klein, Sharma, & Nguyen, 2000 Pointer & Watt, 1987). Here we consider both the effects of separation and spatial scale. Second, we are interested in the perceptual errors (biases or shifts in the point of subjective alignment) that observers make, even in the absence of a phase shift of the neighboring patches (Levi et al., 2003). Large errors have been previously described in amblyopic position and shape judgments (Bedell & Flom, 1981; Demanins & Hess, 1996; Sireteanu, Lagreze, & Constantinescu, 1993). Third, we evaluate the effectiveness of phase-capture and determine the weights given to each of the cues (envelope and carrier) in the perception of shape. In particular, we are interested in whether amblyopes give different weights to these cues than do normal observers.

2. Methods

The methods are identical to those used by Levi et al. (2003), and will be only briefly described here.

2.1. Stimuli

The stimuli are illustrated in Levi et al. (2003, Figs. 1 and 2) and a subset are shown in the inset of Fig. 1. They consisted of strings of 5 circular Gabor patches. Each patch was constructed to have 0.66 carrier cycles per Gaussian envelope standard deviation (σ), corresponding to a spatial frequency bandwidth of 0.825 octaves. The carrier orientation was always aligned with the contour. The patches were briefly presented (≈200 ms) on a Sony Trinitron F520 21″ flat screen monitor at a contrast of 80%, on a mean luminance background (≈80 cd/m^2).

The contours were either a straight line, or a circular arc. We tested observers at one or more viewing distances. The viewing distance was selected to ensure that the stimuli were well within the observers' pass-band: at the closest distance the radius of curvature was 6° and the spatial frequency of the Gabor carrier was 3.33 c/°. At the intermediate distance the radius was 3° and the carrier spatial frequency was 6.67 c/°, and at the largest distance the radius was 2° and the spatial frequency was 10 c/°. At all distances the radius of the circle was 20 periods (lambda) of the Gabor carrier.

The observers' task was to judge whether the center 'test' patch was above or below the contour defined by the four outer patches (which provided samples of the contour). They were told that the contour was either a straight line or a circle. From trial to trial, the phase of the four outer patches was varied: either: (i) all four patches were phase aligned; (ii) patches 2 and 4 (the "inner patches"—see inset in Fig. 1) were shifted downwards by 90°; or (iii) patches 1 and 5 (the "outer patches"—see inset in Fig. 1) were shifted downwards by 90°. In all three cases, the patch centers were perfectly aligned along the contour. At the start of each trial, a reticule was presented to mark the location of the test patch. The reticule disappeared after 300 ms, and was followed immediately by the stimulus. Since we were interested in the perceived position of the central patch relative to the contour, no feedback was provided. In order to minimize bias, all 9 stimulus conditions (3 curvatures [positive, negative and zero, i.e., radius infinity] and 3 phases [all aligned; patches 2 and 4 shifted by 90°; patches 1 and 5 shifted by 90°]) were randomly interleaved in a single run of 450 trials (≈50 trials per condition). In order to avoid using edges or other

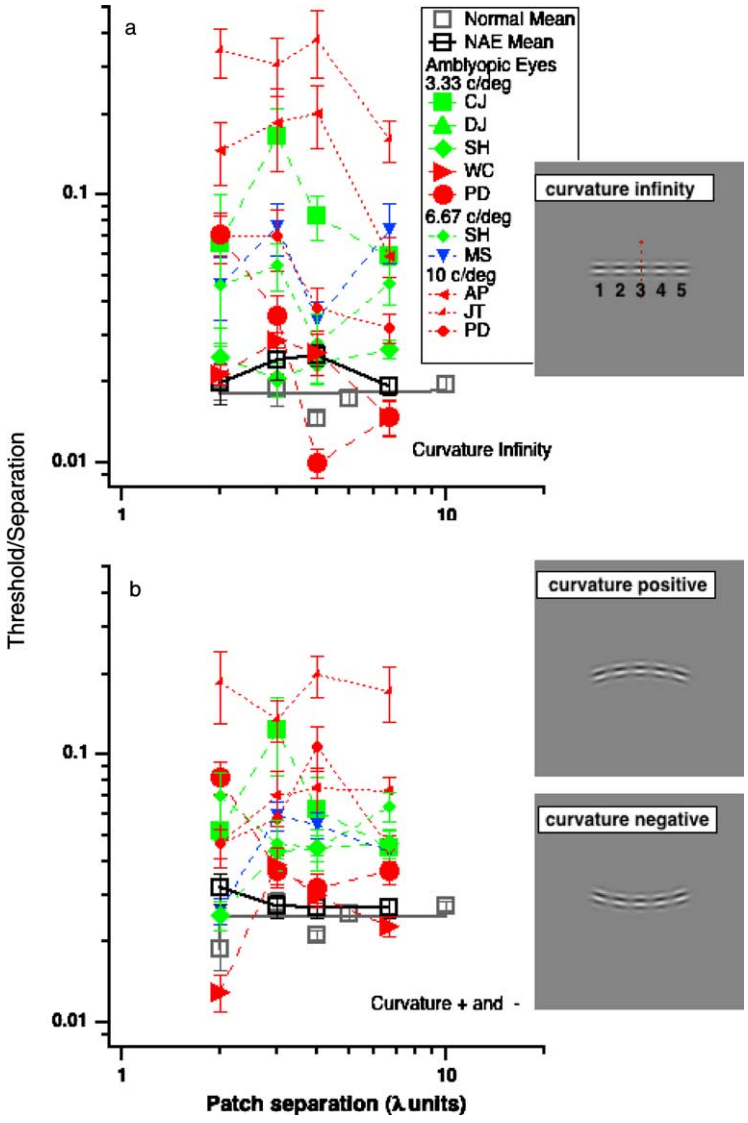

Fig. 1. The insets show examples of our stimuli: a straight line (top), a "frowny face" (middle: i.e., an arc with positive curvature) or a "smiley face" (bottom: i.e., an arc with negative curvature). The observers' task was to judge whether the center 'test' patch (indicated by the arrow) was above or below the contour defined by the four outer patches. From trial to trial, the phase of the four outer patches was varied: all four patches were phase aligned (as illustrated here); or patches 2 and 4 were shifted by 90° or patches 1 and 5 were shifted by 90° but the patch centers were perfectly aligned along the contour. Note that the numbers are for illustration only, and did not appear on the screen. The data shows thresholds (specified as a Weber fraction) for judging the position of the test patch plotted against patch separation for normal observers (open gray squares are the mean of four normal control observers, averaged across viewing distances), the preferred eyes of the amblyopic observers (open black squares) and for the amblyopic eye of each amblyopic observer. In this and subsequent graphs, the type of amblyopia is coded by color (red: strabismic; green: anisometropic and blue for both), and the size of the stimulus is coded by symbol size.

absolute position cues, the orientation of the entire contour (all five patches) was randomly varied (by ±2.5°). From run-to-run, we varied the separation between patches and the viewing distance.

In order to assess the perceived position of the central patch relative to the contour, we used an efficient staircase to control the position of the center 'test' patch. Details of the staircase are given in Levi et al. (2003). The observer responded by pressing one of 4 buttons to indicate both the direction (high or low) and a confidence level. Staircase trials were determined by the observer's prior response (both the direction and confidence). To quantify our results, we constructed psychometric functions from the staircase data and performed Probit analysis to obtain the Point of Subjective Equality (PSE—i.e., the 50% point of the psychometric functions) and the threshold (slope of the psychometric functions). Each condition was repeated at least four times giving approximately 200 trials per condition. The results reported in the figures represent the weighted means of at least four individual estimates obtained from the Probit analyses.

2.2. The "influence function" for sampled shape

We use linear multiple regression to compute the regression coefficients, which correspond to the weights of all cues (C_b, C_{Envout}, C_{Pin} and C_{Pout}) as follows:

$$Off = C_b + C_{Envout}H + C_{Pin}P_{in} + C_{Pout}P_{out} + \varepsilon \quad (1)$$

Off = the measured PSE + sag; where sag is the vertical distance from the center of the envelope of the inner patches to the central sample point of a circle that goes through the center of the envelopes of the inner and outer patches (see Levi et al., 2003, Fig. 8a). C_{Envout} is the coefficient of the location of the envelope of the outer patches relative to the inner patches; C_{Pin} is the coefficient of the carrier phase of the inner patches; C_{Pout} is the coefficient of the carrier phase of the outer patches; C_b is a constant, representing observer bias. The stimulus parameters are H, P_{in} and P_{out}. H is the envelope location of the outer patches (the vertical distance in min of arc between the inner and outer patches), and it is needed to capture the degree of curvature for curved contours; P_{in} and P_{out} are the phase shifts of the inner and outer carrier in min of arc; and ε is the residual error. In our experiments, for a given separation and curvature, we have three values of H ($H = 0$ corresponding to a curvature of zero [radius of curvature = infinity], and a positive and negative H, corresponding to the negative and positive curvatures). For each separation, we computed the weights (coefficients) for each of the three cues. These weights are unitless, and correspond to the gain or influence function of each cue. This influence function may be thought of as the classification image for shape (Levi & Klein, 2002; Levi et al., 2003; Murray et al., 2003).

2.3. Observers

We tested eight amblyopes, four with strabismus (shown by red symbols in all the data figures in Results), three with anisometropia (shown by green symbols) and one with both (shown by blue symbols). Clinical details are provided in Table 1. Note that the acuities listed in Table 1 were determined using a Bailey–Lovie chart, and we specify both the full line letter acuity and the single letter acuity. Not all observers were tested in all conditions. For amblyopic observers the range of distances was limited by the visibility of the patches since we required that the individual patches be at least two times their detection threshold. For normal observers, this task is contrast independent when the stimuli are twice threshold or higher. Thus, only AP, JT and PD could be tested at 10 c/°; SH and MS at 6.67 c/° and CJ, DJ and WC at 3.33 c/°. The four observers from Levi et al. (2003) served as normal controls (all had corrected-to-normal visual acuity). Viewing was monocular.

3. Results

3.1. Precision of shape perception

Previous studies have shown that amblyopes are imprecise in their judgment of position and shape (Demanins & Hess, 1996; Hess et al., 1999; Levi et al., 2000; Pointer & Watt, 1987). In order to assess the precision of our observers' judgments, we calculated their thresholds (based on the slopes of the psychometric functions) for the conditions in which all patches had their phases in alignment (see inset in Fig. 1). In normal vision the precision of shape and

Table 1
Observer characteristics

Observer	Age (years)	Gender	Type	Strabismus (at 6 m)	Eye	Refractive error	Line letter acuity (single letter acuity)[a]
AP	19	F	Strabismic	L EsoT 4^{Δ} and	R	$-1.50/-0.50\times180$	$20/12.5^{-2}$
				L Hyper 2^{Δ}	L	$-0.75/-0.25\times5$	$20/50$ ($20/32^{+1}$)
JT	52	F	Strabismic	L EsoT 5^{Δ}	R	$-1.25/-1.00\times14$	$20/16^{+2}$
					L	$-1.25/-1.00\times7$	$20/63^{-1}$ (20/20)
PD	48	M	Strabismic	L ExoT 30^{Δ}	R	Plano	$20/20^{+2}$
					L	$+1.00/0.50\times95$	$20/32^{-2}$ (20/20)
WC	20	F	Strabismic	R ExoT 20^{Δ} and	R	$+1.50/-1.25\times180$	$20/20^{+2}$
				L HyperT 9^{Δ}	L	$+0.75/-0.50\times180$	20/32 ($20/25^{-2}$)
MS	55	F	Strabismic and anisometropic	Alt. ExoT 18^{Δ}	R	$+2.75/-1.28\times135$	20/40 ($20/25^{+1}$)
					L	-2.00	$20/16^{-2}$
DJ	59	M	Anisometropic	None	R	$+2.25/-0.75\times100$	20/40 ($20/32^{+2}$)
					L	$+0.75$	20/16
SH	27	M	Anisometropic	None	R	$+0.50$	$20/16^{+2}$
					L	$+3.25/-0.75\times60$	$20/63^{-2}$ ($20/63^{+2}$)
CJ	21	M	Anisometropic and refractive	None	R	$-15.00/-1.25\times150$	$20/125^{-4}$($20/125^{+1}$)
					L	-6.00	$20/16^{-2}$

[a] The acuities listed in Table 1 were determined using a Bailey–Lovie chart, and we specify both the full line letter acuity and the single letter acuity.

position perception depends strongly on the separation of the features, so that the threshold is approximately a constant Weber fraction of the feature separation (Levi & Klein, 2000; Levi et al., 2000). Fig. 1 shows that this is approximately true for normal observers for our stimuli, where the normal Weber fraction (threshold/separation) is about 0.018 or 1 part in 55 (open gray squares and dotted line) for the "line" (curvature infinity, Fig. 1a) and about 0.024 or 1 part in 42 (open gray symbols and dotted line) for the "curves" (averaged across the positive and negative curvatures, Fig. 1b). Averaged across observers, the preferred eyes of amblyopes show a similar trend (black open squares and solid line in Fig. 1). In contrast, the amblyopic eyes (solid colored symbols) generally show elevated thresholds (for JT and AP by more than 10-fold for the line [curvature infinity]), and the elevation is generally greatest at the smallest separations (see also Levi et al., 2000). We specified our thresholds as a "Weber" fraction, which in normal observers makes the thresholds independent of viewing distance. Indeed we did not find a strong effect of viewing distance (coded by symbol size in Fig. 1) which changed the patch size, spatial frequency and separation of the patches. For example, although SH showed consistently higher thresholds for the higher spatial frequency condition (Fig. 1a), PD showed similar thresholds, which were as high, or higher at 3.33 c/° than at 10 c/° at the smallest separation.

3.2. Perceptual errors in shape perception

Normal observers show biases when judging our sampled shapes (Levi et al., 2003 and open gray symbols in Fig. 2), which, over the range of separations tested here, are small (less than ≈1/5th of patch wavelength). These biases are evident as shifts in the PSE (about 3% of the stimulus separation for the aligned case). In amblyopes, large shifts in PSE or "spatial distortions" have been previously described (Bedell & Flom, 1981; Demanins & Hess, 1996; Hess et al., 1999; Levi et al., 2000; Pointer & Watt, 1987; Sireteanu et al., 1993). These may correspond to the large biases evident in some of the amblyopic eyes in Fig. 2 (amblyopic eyes are shown by the filled colored symbols). Although both strabismic and anisometropic amblyopes may show larger shifts in PSE than normals, the largest errors are evident in amblyopes with strabismus (strabismic amblyopes JT and AP, and strabismic and anisometropic amblyope MS) who show substantial shifts in PSE, even at small separations. These errors are largest for the curved shapes, and may exceed both the wavelength (left ordinate) and standard deviation (right ordinate) of the patches. We also note that the large scatter in the amblyope's PSE's evident in Fig. 2 and subsequent figures, may be due to their increased thresholds (see Fig. 1).

3.3. Phase capture in shape perception

Our main interest is in determining the effectiveness of phase-capture in amblyopic vision. In order to reveal the influence of carrier phase shifts, we subtract out the PSE when the carrier is aligned with the contour (from Fig. 2) and plot the *change* in PSE induced by the phase shift (Figs. 3 and 4). The top panels in Fig. 3 show the mean data of four normal observers. The top left panel of Fig. 3 shows that shifting the *inner* patches by 0.25 cycle (open symbols) results in almost complete capture (0.25λ—dashed line) at the smallest separation (2λ), and the effect falls off more or less linearly with separation until a near zero effect is reached (although even at 10 λ, the shift of the inner patches results in a small residual change in perceived position). A 0.25 cycle shift of the *outer* pair of patches has a much smaller effect, in the opposite direction (top right panel of Fig. 3).

The lower panels of Fig. 3 show the data of a strabismic amblyope (JT), whose results differed most markedly from normal (but see also the data of AP in the middle panel of Fig. 4). We expected that amblyopes might show reduced capture, and indeed she does show less capture for the curved conditions at small separations (note the scale is three times larger than the top panel); interestingly however, JT's amblyopic eye shows very strong "capture" for the no curvature condition, and the capture is in the wrong direction: repulsion by the inner patches and she also shows attraction by the outer patches. JT's results cannot be explained by low contrast sensitivity, since the capture is almost independent of contrast in normal observers (see Levi et al., 2003, Fig. 6). We note that on questioning, she sometimes reported seeing six (rather than five) patches with her amblyopic eye. "Monocular diplopia" has been previously noted in strabismics (Ramachandran, Cobb, & Levi, 1994), and we suspect that it may be a more common form of spatial distortion in amblyopia with discrete, briefly presented stimuli, than has been reported, much like the distortions recently reported for extended stimuli by Barrett, Pacey, Bradley, Thibos, and Morrill (2003). A detailed report on this observer's perceptual distortions is presented elsewhere (Popple & Levi, in press). However, this distortion of perception would have influenced her alignment judgements both when the patches were all in phase and when they were phase shifted, so any effects of monocular diplopia should have been cancelled out. Rather, it appears that for this observer, at least for the curved contours, the phase of the outer patches strongly influences performance, and the influence of the inner patches is suppressed. We will address these aberrant results further in the Discussion section. The results of the other seven amblyopes are shown in Fig. 4.

None of the other amblyopes show results as extreme as JT. Several show normal or near normal capture by the inner patches, notably DJ and MS. Others show

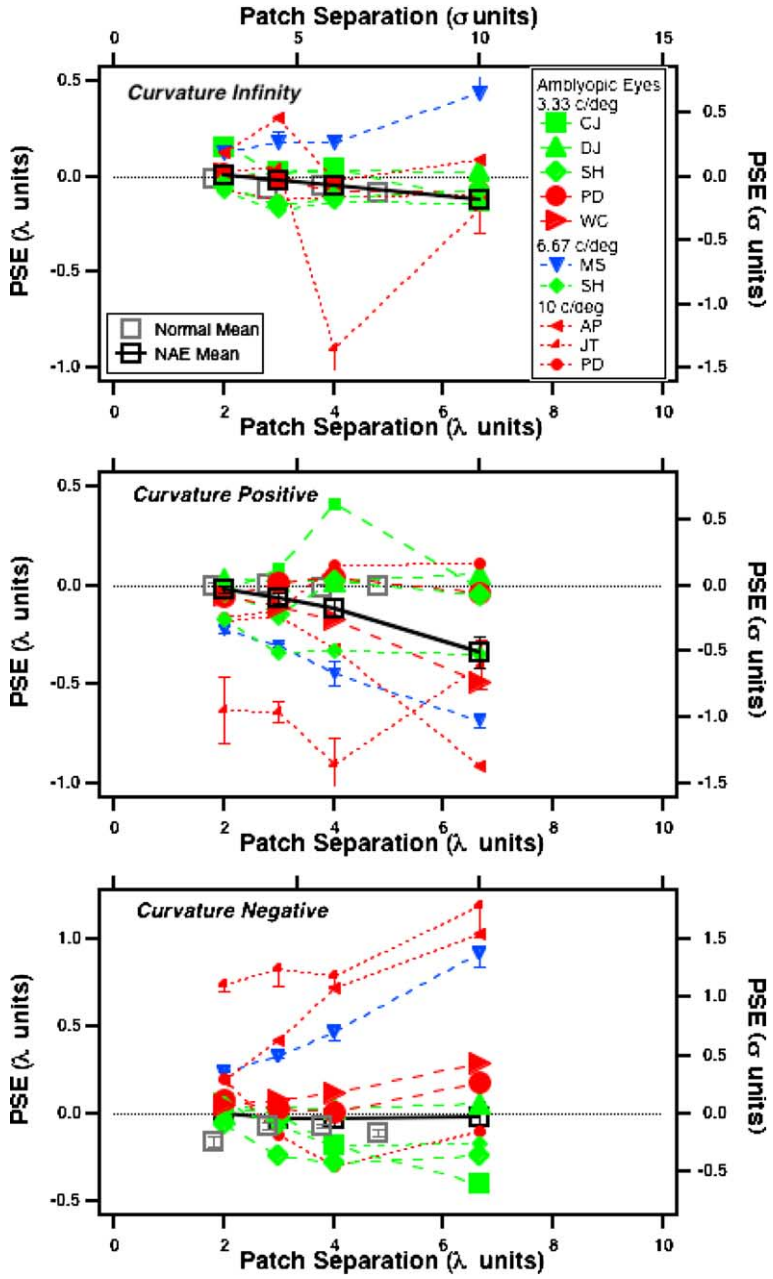

Fig. 2. The PSE (specified in units of the carrier wavelength) is plotted as a function of the patch separation (also specified in units of the carrier wavelength) for each observer when all 5 patches are phase aligned (as in the inset of Fig. 1). All details as in Fig. 1, however, for clarity in this and subsequent figures, we show only representative error bars.

reduced capture at the smallest separations, in particular PD (at both viewing distances), SH for curvature infinity, and CJ for the positive curve. Only AP shows the "repulsion" by inner patches for the negative curvature. Interestingly several of the amblyopic observers show "attraction" (rather than repulsion) by the outer patches.

4. Discussion

We evaluated three aspects of amblyopes' shape perception. First, our results, consistent with a number of previous studies, show that amblyopes are imprecise in shape discrimination, showing elevated thresholds for both lines and curves (Demanins & Hess, 1996; Hess et al., 1999; Levi et al., 2000; Pointer & Watt, 1987). Thresholds may be elevated as much as a log unit or more. Previous studies suggest that position discrimination thresholds may be more compromised in strabismic than in anisometropic observers (Demanins & Hess, 1996; Levi et al., 2000). Surprisingly, in our small sample, there was not a clear distinction based on the type of amblyopia (coded by color in Fig. 2): both strabis-

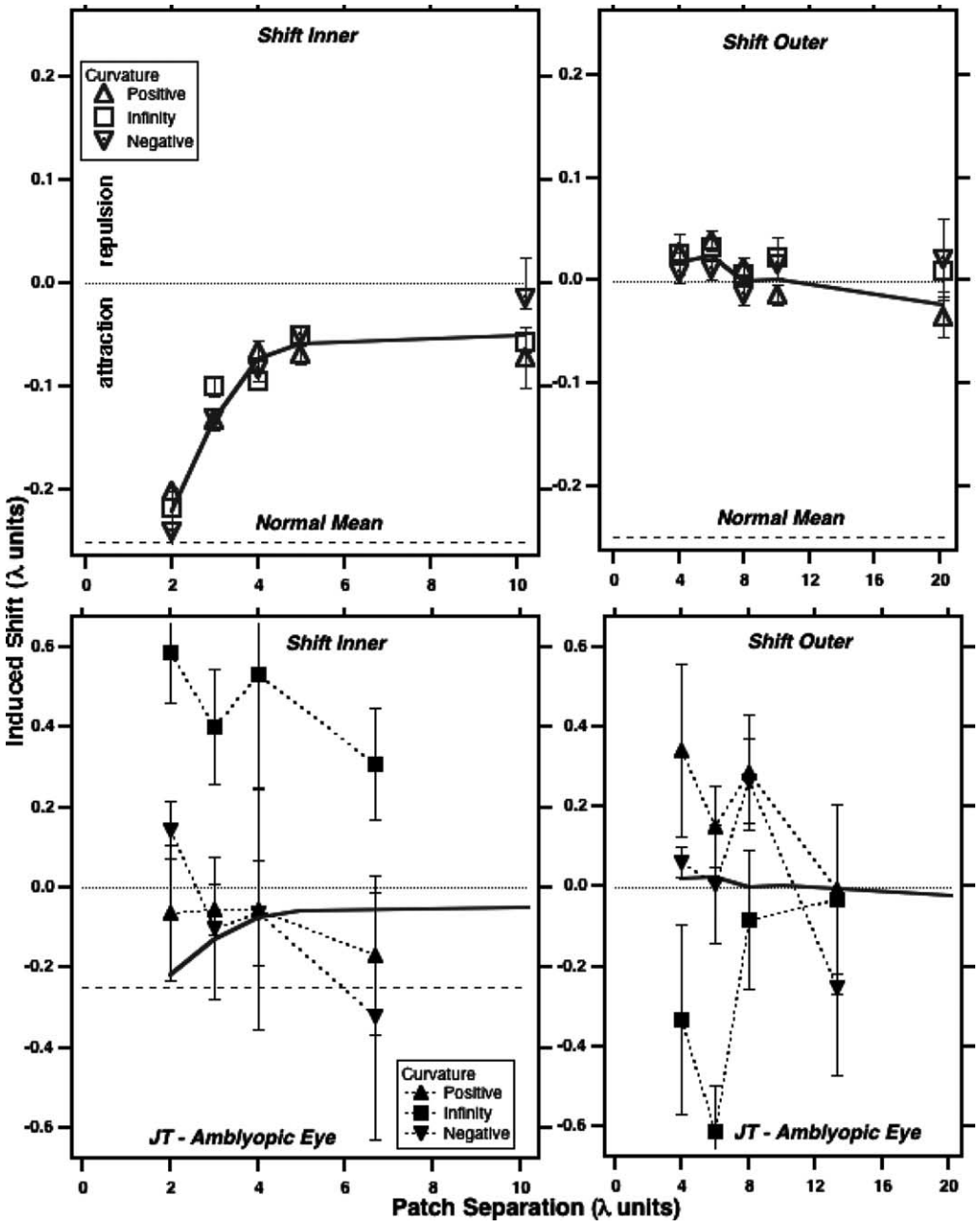

Fig. 3. The induced shift vs patch separation. i.e., the *change* in PSE induced by the phase shift (i.e., we subtract out the PSE's shown in Fig. 2). The top panels show the data of 4 normal observers, averaged across viewing distances and observers. The left panel shows the effect of shifting the "inner patches (inset), the right panel the effect of shifting the outer patches. The dotted line at 0.0 indicates no induced phase shift, the dashed line at -0.25λ indicates complete phase capture. Note that the squares are for the "line" (curvature infinity) and the triangles for the positive and negative curvatures. The bottom panels show data of the amblyopic eye of a strabismic amblyope. Note that the vertical scale is expanded by a factor of three in the lower panels—to facilitate comparison with the normal observers, the best fitting line through the normal data is shown (gray dotted line) in the lower panel.

mics (red) and anisometropes (green) showed elevated thresholds. However, in order to examine the role of visual acuity we replotted each observer's threshold as a function of their visual acuity (full line letter acuity, which reflects crowding) in Fig. 5. Specifically, Fig. 5 shows each observer's threshold at the largest separation (6.66λ in order to minimize the effect of crowding or lateral interactions on threshold), averaged across the three curvatures. Note that the anisometropes all have similar thresholds, despite an approximately 4-fold acuity range. Interestingly for the strabismic observers, there appears to be a strong relationship between acuity and threshold, with JT showing the worst acuity of the strabismic observers and the highest thresholds. It is also

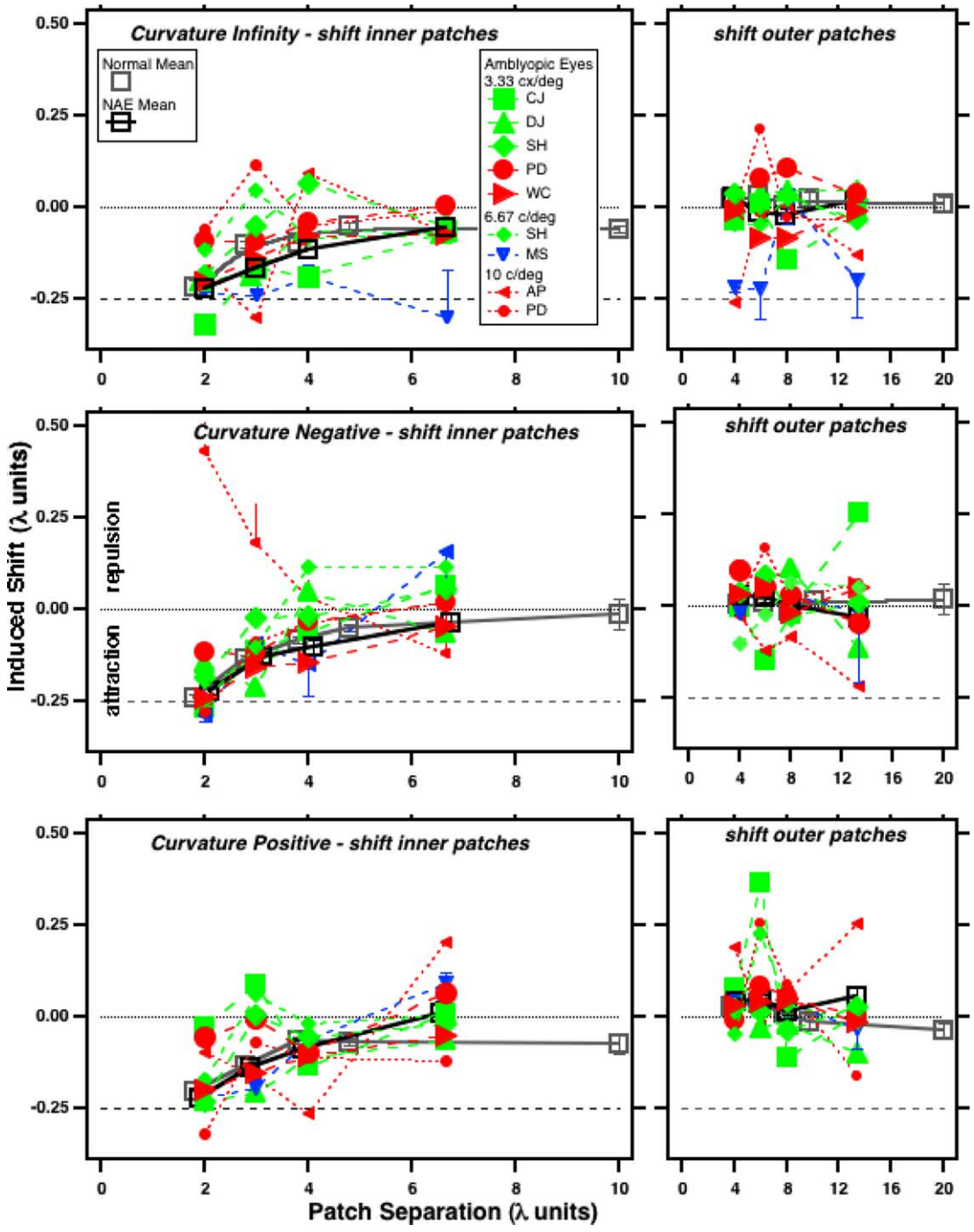

Fig. 4. The induced shift (left ordinate) vs patch separation for the other amblyopic observers. The top panels are for the "line" (curvature infinity) and the lower panels for the positive and negative curves. The details are as in Fig. 1.

interesting to note, that JT has substantially higher thresholds than anisometropes SH and CJ who have equal or poorer acuity. Below, we speculate about a possible role for crowding and/or abnormal lateral interactions. We note that our sample size is small, and as shown by a recent large-scale study (McKee, Levi, & Movshon, 2003) one must exercise caution in generalizing to the amblyopic population as a whole.

Second, we found that amblyopes often have much larger biases than do normal observers (Bedell & Flom, 1981; Demanins & Hess, 1996; Levi et al., 2003; Sireteanu et al., 1993). These biases tend to be largest for curved shapes and at large separations, and appear to be rather idiosyncratic.

Third, we evaluated the effectiveness of phase-capture in the perception of shape. The results of our amblyopic

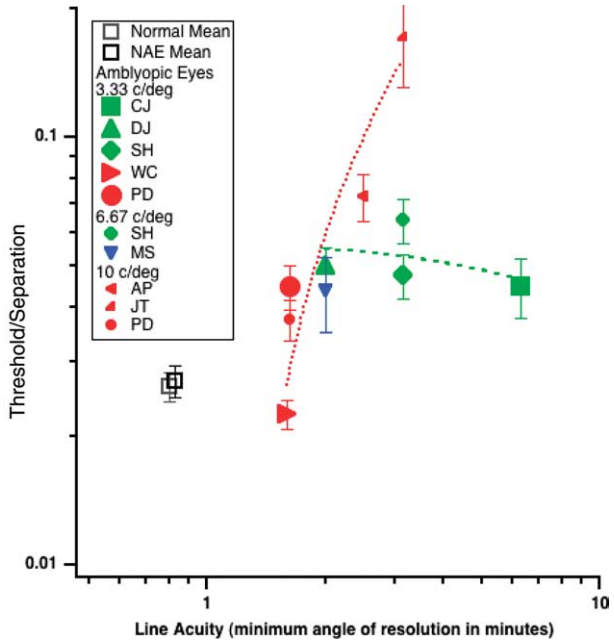

Fig. 5. Threshold at the largest separation (6.66λ), averaged across the three curvatures (from Fig. 1a and b) versus full line letter acuity (in minutes). The strabismic (red) and mixed (blue) amblyopes show a strong relationship between acuity and threshold. The lines are the best fitting regression lines to the data of the pure anisometropes (green) and all strabismics (i.e., the four pure strabismics and the strabismic anisometrope: red).

observers were surprising. Our expectation was that amblyopes might be "phase blind", since several studies suggest that amblyopes may be much less sensitive to relative spatial phase (Lawden et al., 1982; Pass & Levi, 1982) and to phase-shift induced alterations in perceived orientation (Popple & Levi, 2000b). Indeed, several amblyopic observers did show reduced capture by the phase of the inner patches. However, several of the amblyopes were more sensitive to the phase of the outer patches than were the normals (e.g. Fig. 3). Thus, the failure of amblyopes to perceive certain orientation illusions (e.g. Popple & Levi, 2000b) may be a consequence of abnormal weighting of the cues rather than to reduced phase insensitivity.

In our experiments, the contour is defined by two cues—the cue provided by the Gabor carrier (the 'carrier' cue) and that defined by the Gaussian envelope (the 'envelope' cue). The variance in each of these cues predicts our results for normal observers quite accurately (Levi, Hariharan, & Klein, 2002). Below we estimate how the amblyopic visual system weights each of the cues.

4.1. Weighting of visual cues for shape perception: the amblyopic "influence function" for sampled shape

We are interested in how each cue to the sample position is weighted by the amblyopic visual system to provide an estimate of contour shape. Using linear multiple regression, Levi et al. (2003) showed that it is possible to estimate the weights by computing the regression coefficients, which correspond to the weights, of all cues (see Section 2). This influence function may be thought of as the classification image for shape (Levi & Klein, 2002, Murray et al., 2003; Levi et al., 2003).

Fig. 6 shows the weights C_{Pin} (top panel), C_{Pout} (middle panel), C_{Envout} (bottom panel) for each of the amblyopic observers. The top panel confirms that several amblyopes (JT, AP, PD and CJ) place lower weights on the phase of the inner patches, particularly at the smallest separations. In normal observers the outer patch carrier (middle panel) has a small but significant weighting (≈ -0.1), in the opposite direction from that of the inner patches (i.e., repulsion), which also decreases with separation. However, the middle panel also shows that several amblyopes (MS, WC, JT and AP), show a strong influence (in the wrong direction) of the phase of the outer patches. That is, they show attraction rather than repulsion. The bottom panel shows C_{Envout} plotted as a function of separation. The data for the normal observers and for the non-amblyopic eyes fall close to the blue dotted line showing the predicted weighting of the envelope of the outer patches if the observer sets the test patch (envelope center) on a circular contour. Interestingly most of the anisometropic amblyopes and strabismic amblyope PD, show similar weighting of the outer envelope cue. This predicted weighting is approximately -0.33. Settings above the blue dotted line reflect oblate errors (squashed circle), while settings below the blue dotted line reflect prolate errors (pointy circle). Most of the strabismics show oblate errors, most notably JT, MS and AP show envelope weights that fall close to the dotted line at $C_{\mathrm{Envout}} = 0$, indicating performance if the observer completely ignored the outer patches. Note that at a separation of 4λ units, JT's data approach the solid black line at $C_{\mathrm{Envout}} = 0.5$ indicating performance if the observer set the test patch to line up with the average of the inner and outer envelope positions. An ordinate value of -1 (not shown) would correspond to the extreme prolate case of a "V". While several amblyopes make small prolate errors (CJ, DJ, SH [at 3.33 c/°]) none show extreme errors in this direction. A value of $C_{\mathrm{Envout}} = 1$ (red dashed line) indicates performance if the observer completely ignored the inner patches and the setting of the test patch was completely determined by the envelope of the outer patches.

To facilitate a comparison of the envelope cue weightings of amblyopes with those of normal observers, we replot in Fig. 7 the weights from the lower two panels of Fig. 6, plotting C_{Pout} against C_{Envout} with an expanded scale. The envelope weights of normal observers are almost invariant to separation, occupying a very narrow range, from about -0.32 to -0.42 along the ordinate. Similarly, in normal observers, the weights

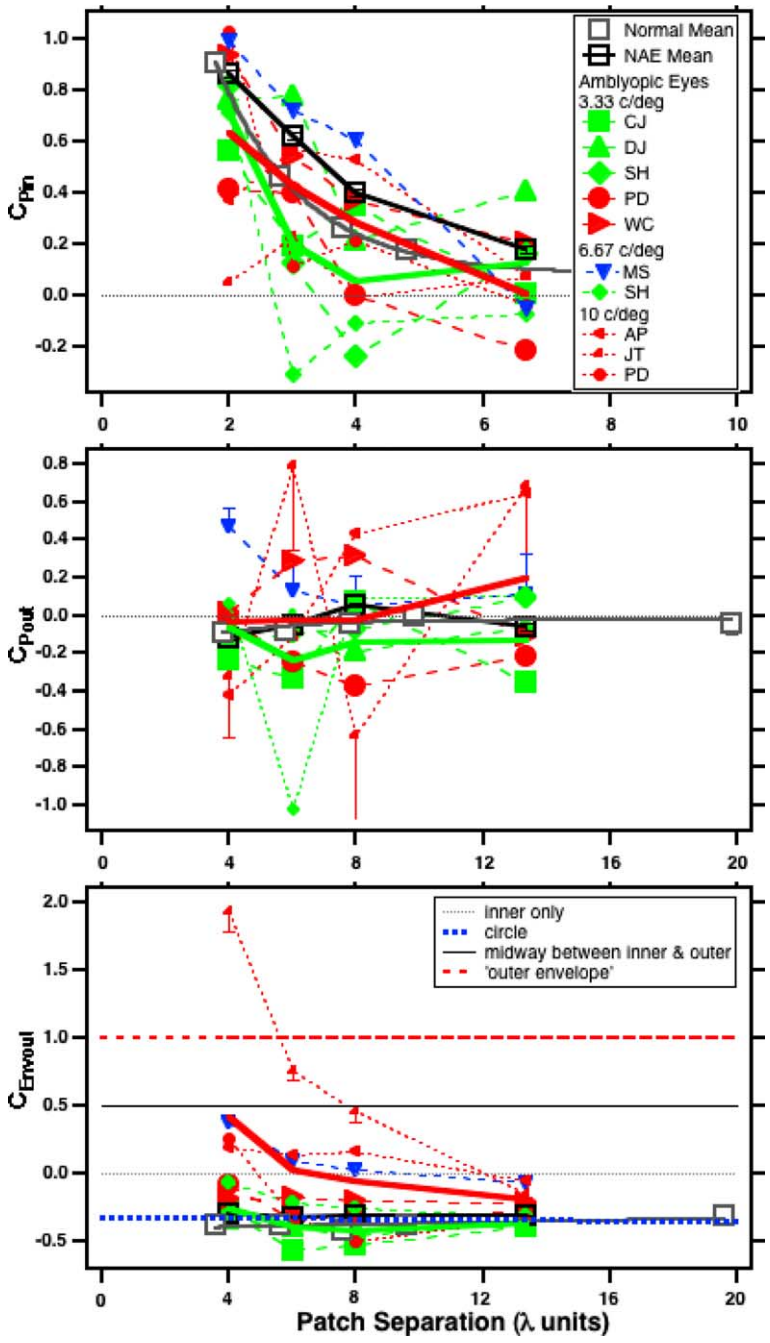

Fig. 6. Regression coefficients showing the weighting of the inner (C_{Pin}: top panel) and outer (C_{Pout}: middle panel) patch carriers, and the weighting of the envelope of the outer patches (C_{Envout}: bottom panel) plotted as a function of separation. The details are generally as in Fig. 1. The thick red and green lines show the mean data of strabismic and anisometropic amblyopes respectively. In the lower panel the gray dotted line at $C_{Envout} = 0$ indicates performance if the observer completely ignored the outer patches (i.e., if the setting of the test patch were completely determined by the envelope of the inner patches). The solid black line at $C_{Envout} = 0.5$ indicating performance if the observer set the test patch to line up with the average of the inner and outer envelope positions. The dotted blue line at C_{Envout} approximately -0.33 shows the predicted weighting of the envelope of the outer patches if the observer set the test patch on the contour. The dashed red line at $C_{Envout} = 1$ (red dashed line) indicates performance if the observer completely ignored the inner patches and the setting of the test patch was completely determined by the envelope of the outer patches.

for the outer patch carrier (C_{Pout}) occupy a narrow range from near zero to about -0.1 along the ordinate. Thus, all of the normal eye data are contained within the gray square. Several of the strabismic amblyopes show values much higher (WC, AP, JT and MS) and also much lower (PD, JT) values, consistent with the notion that the inner patches may be suppressed or crowded. Note that we have truncated the ordinate range in this graph, so it does not show the extreme point at almost 2 for JT. The differences between strabismics and an-

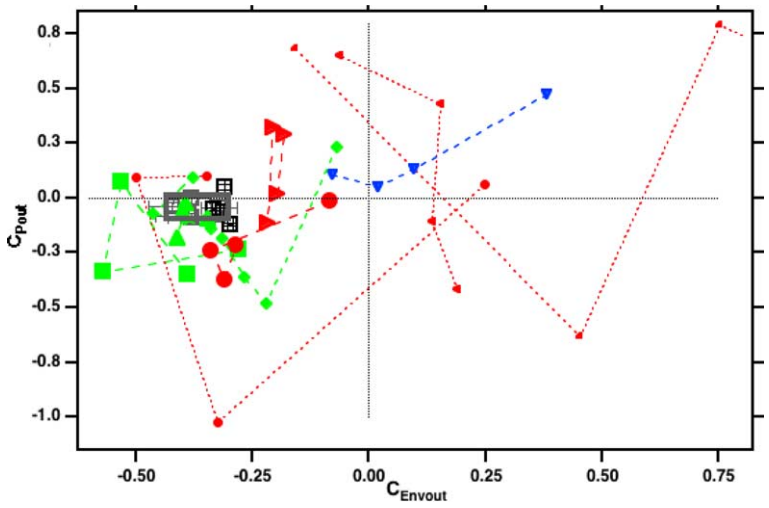

Fig. 7. This figure replots the weights from Fig. 5, plotting C_{Pout} against C_{Envout}. Note that we have truncated the ordinate range in this graph, so it does not show the extreme point at almost 2 for JT. The black dotted vertical and horizontal lines show C_{Pout} and C_{Envout} equal to zero. The gray box contains the complete range of normal data. The main purpose of this figure is to show the scatter of the amblyopes data relative to the normal controls.

isometropes are also evident in their mean data, shown in Fig. 6 by the thick red and green lines respectively.

Our results suggest that amblyopes are not phase blind; however, they are less sensitive to changes in spatial phase than normals (Lawden et al., 1982; Pass & Levi, 1982). An ideal observer would weight the cues by their inverse variance, so that the more reliable cues are given a stronger weight,and we showed that the variance in each of the cues predicts our results for normal observers quite accurately (Levi et al., 2003). The abnormal influence functions of our amblyopes show that they apply different weightings to the cues for shape than do normal observers. A number of our observers show a weaker influence of the phase of the inner patches, and a stronger influence of both the phase and envelope of the outer patches. Below, we speculate that this may be a consequence of abnormal "crowding" of the inner patches by the outer ones (Bonneh, Sagi, & Polat, 2004; Levi et al., 2002).

Consider the data of JT in the lower panel of Fig. 6. At the largest separation, her weighting of the outer patch envelope (C_{Envout}) was −0.16, so with widely spaced samples, all of the samples were taken into account, and she perceived the shape as an oblate circle. At the second largest separation, the envelope weighting was 0.45, approximately the average of the inner and outer envelope positions. In contrast, at the two smallest separations, her weighting of the outer envelope increased steeply to 0.75 and then 1.93, as if the inner patches were completely ignored ($C_{Envout} = 1$). Can these results be explained on the basis of crowding and/or abnormal lateral interactions? It is well known clinically that some amblyopes show much more impairment for a line of letters than for a single letter—i.e., that amblyopes show a crowding effect, and a recent large scale study (Bonneh et al., 2004) suggests that this crowding is much more marked in strabismic (or mixed) than in pure anisometropic amblyopes. Moreover, they found that among strabismic amblyopes there was a strong correlation between the crowding effect and "lateral suppression" (contrast threshold elevation for detection of a Gabor patch by neighboring flanks). Thus, it is reasonable to ask whether in our experiments, the outer patches might have suppressed or crowded the inner ones as the separation decreased, rendering them ineffective as samples for judging the shape. In order to address this we calculated a "crowding index" by taking the ratio of the observers' full line letter acuity (in minutes) to their single letter acuity (in minutes).

Fig. 8 plots C_{Pin} and C_{Envout} (at the mean of the two smallest separations) as a function of the amount of crowding, as indicated by the crowding index. For the 4 anisometropes, the crowding index was near one, whereas for the strabismic amblyopes it ranged up to over three, consistent with the large population of Bonneh et al. (2004). The strabismic amblyope with the strongest crowding (JT) showed the smallest weighting for the phase of the inner patches (C_{Pin}) and the largest weighting for the envelope of the outer patches (C_{Envout}), and the other strabismics, with less extreme crowding, have values between those of the anisometropes and JT, consistent with an explanation based on crowding or lateral suppression of the inner patches by the outer ones. The lower panel of Fig. 8 is particularly telling. It shows that for the strabismics, the deviation of the weighting of the relative locations of the inner and outer envelopes at small separations is directly related to the crowding index. For several of the anisometropes who show little crowding, C_{Envout} is close to the "expected" normal value of −0.33, for judging

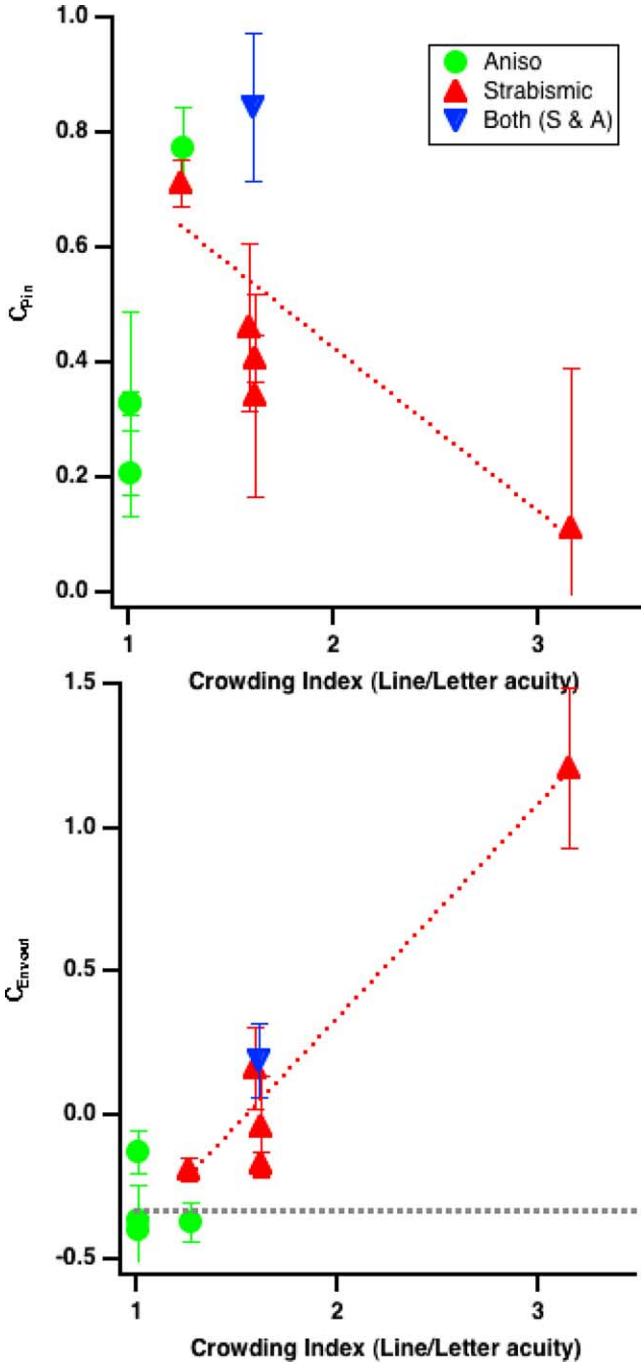

Fig. 8. C_{Pin} and C_{Envout} at the two smallest separations, are plotted as a function of the amount of crowding, as indicated by the crowding index (the ratio of full line letter acuity (in minutes) to single letter acuity (in minutes). For the four anisometropes (green), the crowding index was near one, whereas for the strabismic (red) amblyopes it ranged up to over three. For the strabismics, the weighting for the phase of the inner patches (C_{Pin}: top panel) is inversely proportional to crowding, and the weighting of the envelope of the outer patches (C_{Envout}: lower panel), is proportional to the crowding index. In the lower panel the gray horizontal line at −0.33 shows the "expected" value for normal observers if the observer set the test patch on the contour (which was close to their measured value). The red and green lines are the best fitting regression lines for the strabismic and anisometropic observers respectively.

a circle using all of the available samples. In contrast, for the strabismic with the strongest crowding, C_{Envout} is close to one, as if she used only the outer envelope.

Acknowledgement

We are grateful to Hope Queener for programming the experiments. This research was supported by Research grants R01EY01728 and RO1EY04776.

References

Barrett, B. T., Pacey, I. E., Bradley, A., Thibos, L. N., & Morrill, P. (2003). Nonveridical visual perception in human amblyopia. *Investigative Ophthalmolology & Visual Science, 44*, 1555–1567.

Bedell, H. E., & Flom, M. C. (1981). Monocular spatial distortion in strabismic amblyopia. *Investigative Ophthalmolology & Visual Science, 20*, 26–28.

Bonneh, Y. S., Sagi, D., & Polat, U. (2004). Local and non-local deficits in amblyopia: acuity and spatial interactions. *Vision Research, 44*, 3099–3110.

Demanins, R., & Hess, R. F. (1996). Positional loss in strabismic amblyopia—interrelationship of alignment threshold, bias, spatial scale and eccentricity. *Vision Research, 36*, 2771–2794.

Ernst, M. O., & Banks, M. S. (2002). Humans integrate visual and haptic information in a statistically optimal fashion. *Nature, 415*, 429–433.

Hess, R. F., Wang, Y. Z., Demanins, R., Wilkinson, F., & Wilson, H. R. (1999). A deficit in strabismic amblyopia for global shape detection. *Vision Research, 39*, 901–914.

Hillis, J. M., Ernst, M. O., Banks, M. S., & Landy, M. S. (2002). Combining sensory information: mandatory fusion within, but not between, senses. *Science, 298*, 1627–1630.

Jacobs, R. A. (2002). What determines visual cue reliability. *Trends in Cognitive Sciences, 6*, 345–350.

Landy, M. S., Maloney, L. T., Johnston, E. B., & Young, M. (1995). Measurement and modeling of depth cue combination: in defense of weak fusion. *Vision Research, 35*, 389–412.

Lawden, M. C., Hess, R. F., & Campbell, F. W. (1982). The discriminability of spatial phase relationships in amblyopia. *Vision Research, 22*, 1005–1016.

Levi, D. M., Hariharan, S., & Klein, S. A. (2002). Suppressive and facilitatory interactions in amblyopic vision. *Vision Research, 42*, 1379–1394.

Levi, D. M., & Klein, S. A. (2000). Seeing circles. *Vision Research, 40*, 2329–2339.

Levi, D. M., & Klein, S. A. (2002). Classification images for detection and position discrimination in the fovea and parafovea. *Journal of Vision, 2*, 46–65.

Levi, D. M., Klein, S. A., Sharma, V., & Nguyen, L. (2000). Detecting disorder in spatial vision. *Vision Research, 40*, 2307–2327.

Levi, D. M., Li, R., & Klein, S. A. (2003). "Phase capture" in the perception of interpolated shape: cue combination and the influence function. *Vision Research, 43*, 2233–2243.

McKee, S. P., Levi, D. M., & Movshon, J. A. (2003). The nature and variety of visual deficits in amblyopia. *Journal of Vision, 3*, 380–405.

Murray, R. F., Sekuler, A. B., & Bennett, P. J. (2003). A linear cue combination framework for understanding selective attention. *Journal of Vision, 3*, 116–145.

Pass, A. F., & Levi, D. M. (1982). Spatial processing of complex stimuli in the amblyopic visual system. *Investigative Ophthalmolology & Visual Science, 23*, 780–786.

Pointer, J. S., & Watt, R. J. (1987). Shape recognition in amblyopia. *Vision Research, 27*, 651–660.

Popple, A. V., & Levi, D. M. (2000a). A new illusion demonstrates long-range processing. *Vision Research, 40*, 2545–2549.

Popple, A. V., & Levi, D. M. (2000b). Amblyopes see true alignment where normal observers see illusory tilt. *Proceedings of the National Academy of Science, 97*, 11667–11672.

Popple, A. V., & Levi, D. M. (2004). Combining cues in contour orientation. *Vision Research, 44*, 3081–3090.

Popple, A. V., & Levi, D. M. (in press). Location coding by the human visual system: multiple topological adaptations in a case of strabismic amblyopia. *Perception*.

Popple, A. V., & Sagi, D. (2000). A Fraser illusion without local cues. *Vision Research, 40*, 873–878.

Ramachandran, V. S., Cobb, S., & Levi, L. (1994). The neural locus of binocular rivalry and monocular diplopia in intermittent exotropes. *Neuroreport, 5*, 1141–1144.

Simmers, A. J., & Bex, P. J. (2004). The representation of global structure in amblyopia. *Vision Research, 44*, 523–533.

Sireteanu, R., Lagreze, W. D., & Constantinescu, D. H. (1993). Distortions in two-dimensional visual space perception in strabismic observers. *Vision Research, 33*, 677–690.

Watt, R. J., Ward, R. M., & Casco, C. (1987). The detection of deviation from straightness in lines. *Vision Research, 27*, 1659–1678.

Wilkinson, F., Wilson, H. R., & Habak, C. (1998). Detection and recognition of radial frequency patterns. *Vision Research, 38*, 3555–3568.

Young, M. J., Landy, M. S., & Maloney, L. T. (1993). A perturbation analysis of depth perception from combinations of texture and motion cues. *Vision Research, 33*, 2685–2696.

Zanker, J. M., & Quenzer, T. (1999). How to tell circles from ellipses: perceiving the regularity of simple shapes. *Naturwissenschaften, 86*, 492–495.